ORIGINAL ARTICLE

CrossMark

Neuroprotective activity of leukemia inhibitory factor is relayed through myeloid zinc finger-1 in a rat model of stroke

Stephanie M. Davis[1] · Lisa A. Collier[1] · Elspeth A. Foran[2] · Christopher C. Leonardo[3] · Craig T. Ajmo Jr[3] · Keith R. Pennypacker[1,4]

Abstract
The aim of this study was to determine whether leukemia inhibitory factor (LIF) exerts its neuroprotective effects through signal transduction of the transcription factor myeloid zinc finger-1 (MZF-1). According to the hypothesis of this study, MZF-1 mediates LIF-induced neuroprotective signaling during ELVO through increased expression and transcriptional activity. To determine the in vivo role of MZF-1 in LIF-induced neuroprotection, we used Genomatix software was used to MZF-1 sites in the promoter region of the rat superoxide dismutase 3 (SOD3) gene. Stroke was induced via middle cerebral artery occlusion, and animals were administered PBS or 125 μg/kg LIF at 6, 24, and 48 h after the injury. MZF-1 binding activity was measured using electrophoretic mobility shift assay (EMSA) and its expression/localization were determined using western blot and immunohistochemical analysis. To determine whether MZF-1 relays LIF-induced neuroprotection in vitro, primary cultured neurons were subjected to oxygen-glucose deprivation (OGD) after treatment with PBS or LIF. MZF-1 expression was measured in vitro using real time PCR and immunohistochemical staining. Transfection with siRNA was used to determine whether LIF protected cultured neurons against OGD after silencing MZF-1 expression. Four MZF-1 binding sites were identified by Genomatix, and EMSA confirmed in vivo binding activity in brain after MCAO. LIF significantly increased MZF-1 protein levels compared to PBS treatment at 72 h post-MCAO. In vivo nuclear localization of MZF-1 as well as co-localization of SOD3 and MZF-1 was observed in the cortical neurons of LIF-treated rats. Primary cultured neurons treated with LIF had significantly higher levels of MZF-1 mRNA and protein after LIF treatment compared to neurons treated with PBS. Finally, knockdown MZF-1 using siRNA counteracted the neuroprotective effects of LIF in vitro. These data demonstrate that LIF-mediated neuroprotection is dependent upon MZF-1 activity. Furthermore, these findings identify a novel neuroprotective pathway that employs MZF-1, a transcription factor associated with hematopoietic gene expression.

Keywords Transcription factors · Ischemia · Stroke · Antioxidants · Cytokines · Neurosurvival

Abbreviations
ELVO	emergent large vessel occlusion
EVT	endovascular thrombectomy
LDH	lactate dehydrogenase
LIF	leukemia inhibitory factor
MCAO	middle cerebral artery occlusion
MZF-1	myeloid zinc finger-1
NeuN	neuronal nuclear antigen
SOD3	superoxide dismutase 3
TF	transcription factor
tPA	tissue plasminogen activator

✉ Keith R. Pennypacker
keith.pennypacker@uky.edu

1 Department of Neurology, University of Kentucky, 741 S. Limestone BBSRB Room B457, Lexington, KY 40536-0509, USA

2 Department of Molecular Medicine, University of South Florida, Tampa, FL, USA

3 Department of Molecular Pharmacology and Physiology, University of South Florida, Tampa, FL, USA

4 Department of Neuroscience, University of Kentucky, Lexington, KY, USA

Introduction

Ischemic stroke remains the fifth leading cause of death in the United States as well as a major cause of adult disability (Talwalkar et al. 2015). Of the patients affected by

acute ischemic stroke, approximately 35% have an emergent large vessel occlusion (ELVO), which involves the blockage of a major brain artery such as the internal carotid artery or the most proximal segment of the middle cerebral artery (MCA) (Hastrup et al. 2016). Treatment with thrombolytic agents, such as tissue plasminogen activator, may be sufficient for attenuating neurological damage during the early phases of stroke pathology (Hacke et al. 2008). However, a report from the 2017 International Stroke Conference revealed that only 3.8% of eligible patients receive intravenous tPA within the therapeutic window (Madsen et al. 2017).

Performing endovascular thrombectomy (EVT), which involves the mechanical removal of thrombi using a stent retriever, on stroke patients who are either ineligible or non-responsive to tPA administration alone has increased recanalization rates in 69.5% of ELVO patients (Dirnagl et al. 1999; Smith et al. 2008). According to the results of the HERMES meta-analysis, which reviewed the results of several clinical trials involving the use of EVT, this procedure yielded significant recovery among patients who underwent randomization ≥5 h after the onset of stroke and patients who were ineligible for tPA (Goyal et al. 2016). As a result, the 2018 Guidelines for patients with acute ischemic stroke have implemented the following eligibility criteria for EVT: a pre-stroke modified Rankin scale between 0 and 1, an NIH Stroke Scale of ≥6, patient age is ≥18, computed tomography (CT) shows ischemic damage in no more than 4 areas of the MCA territory, ability to begin EVT ≥ 6 h after symptom onset, and confirmed blockage of the internal carotid artery or the most proximal segment of the MCA (Barber et al. 2000; Powers et al. 2018). Unfortunately, not all ELVO patients meet these eligibility criteria for EVT (McMeekin et al. 2017). These patients remain vulnerable to delayed brain damage in the ischemic penumbra, which begins within hours after the onset of stroke (Dirnagl et al. 1999; Leonardo and Pennypacker 2011). The lack of treatment options for these patients with permanent stroke creates a need for novel therapeutics that will promote cellular survival in the ischemic penumbra.

Leukemia inhibitory factor (LIF) is a cytokine that modulates inflammation and promotes neural cell survival (Azari et al. 2001; Butzkueven et al. 2002; Hendriks et al. 2008; Marriott et al. 2008). LIF is effective in reducing tissue damage and promoting functional recovery after permanent middle cerebral artery occlusion, a rodent model of ELVO. Futhermore, LIF promotes cell survival and antioxidant gene expression in neurons and oligodendrocytes during oxygen-glucose deprivation, an in vitro model of cerebral ischemia (Rowe et al. 2014; Davis et al. 2017). Signaling of LIF occurs via binding to a heterodimeric receptor containing the LIF receptor subunit and transmembrane receptor glycoprotein 130 (Ip et al. 1992). The protein kinase Akt is a critical component of this neuroprotective signaling, which results in transcription of antioxidant genes that are responsible for the neural cell protection after stroke (Suzuki et al. 2005; Rowe et al. 2014; Davis et al. 2017).

However, the transcription factors (TFs) that are activated by Akt and initiate transcription of antioxidant genes have not been defined. The promoter regions of these antioxidant genes contain GC-rich regions as well as binding sites for myeloid zinc finger 1 (MZF-1) (Rowe, Leonardo et al. 2010). MZF-1 belongs to the Kruppel family of TFs and is highly expressed by cells of myeloid origin (Hromas et al. 1991). Although previously implicated in hematopoietic development, MZF-1 modulates expression of several genes that play a role in stroke pathogenesis/recovery (Morris et al. 1995; Hromas et al. 1996a).

Zelko et al. previously showed that MZF-1 regulates expression of superoxide dismutase 3 (SOD3), a secreted antioxidant enzyme (Zelko and Folz 2003, 2004). Although neurons do not express high levels of SOD3 under normal physiological conditions, cortical neurons increase the gene expression of SOD3 as an endogenous defense mechanism against ischemia (Strålin et al. 1995; Fukui et al. 2002; Zelko et al. 2002). LIF protects cortical neurons from ischemia by increasing expression of SOD3 at 72 h after MCAO. The upregulation of SOD3 and other antioxidant genes by LIF promotes improvements in motor skills and reduces tissue damage from oxidative stress (Davis et al. 2017).

Since the upregulation of neuronal SOD3 and improvements in post-stroke motor function are observed at 72 h after MCAO, the goal of this study was to determine whether LIF induces neuroprotective signaling through MZF-1 expression and activity. This report tested the hypothesis that MZF-1 mediates LIF-induced neuroprotective signaling during ELVO through increased expression and transcriptional activity. This hypothesis will be tested using several in vivo and in vitro techniques. To test this hypothesis in vivo, ELVO was simulated using the permanent intraluminal rat model of MCAO. MZF-1 binding sites within the SOD3 promoter were identified using Genomatix software and binding activity as confirmed using electrophoretic mobility shift assay. Protein expression and localization of MZF-1 was determined using western blot and immunohistochemical staining. Real time PCR and immunohistochemistry were used to determine whether MZF-1 expression was altered in cultured neurons after in vitro oxygen-glucose deprivation (OGD). Finally, siRNA-mediated gene silencing was used to determine whether in vitro knockdown of MZF-1 counteracts LIF-mediated neuroprotection.

Experimental procedures

Animal care

Animal procedures were performed according to the NIH Guide for the Care and Use of Laboratory Animals and pre-approved by the Institutional Animal Care and Use Committee at the University of South Florida. The minimum number of animals needed for each study was determined a priori using power analysis. All in vivo procedures were performed on 3-month-old male Sprague–Dawley rats (300–350 g) purchased from Envigo (Indianapolis, IN, USA; RRID:RGD_10395233). Animals were maintained on a 12 h light–dark cycle (07:00–19:00 h) in a climate-controlled room. Animas were allowed access to food and water ad libitum. Cultured neurons were isolated from embryonic day 18 (E18) Sprague-Dawley fetal rat pups.

Middle cerebral artery occlusion

The permanent middle cerebral artery occlusion (MCAO) method, which was used as a model of ELVO in rodents, was performed as previously described (Ajmo et al. 2006). Subsequent reduction in cerebral blood flow was confirmed using Laser Doppler Measurement (Moore Lab Instruments, Farmington, CT). Only animals with a ≥ 60% reduction in cerebral perfusion were included in the study. Animals subjected to the sham MCAO procedure underwent exposure of the common carotid artery without cutting the external carotid or occluding the MCA.

Drug administration

Rats were treated prophylactically with ketoprofen (10 mg/kg s.c.), atropine (0.25 mg/kg s.c.) with two additional doses of ketprofen at 24 and 48 h post-MCAO to control for post-surgical pain. Animals were randomly assigned to receive recombinant human LIF (125 μg/kg i.v.; ProSpec, Ness Ziona, Israel) or PBS (pH 7.4) treatment at 6, 24, and 48 h post-MCAO as previously described (Rowe et al. 2014; Davis et al. 2017). All lab personnel administering drugs were blinded to drug treatments.

Tissue collection

Rats were euthanized at 72 h post-MCAO via intraperitoneal injection of ketamine/xylazine (75 mg/kg and 7.5 mg/kg) as previously described (Ajmo et al. 2006; Seifert et al. 2012) before perfusion of tissues. Tissue was collected and preserved for biochemical and immunohistochemical analysis as previously described (Leonardo et al. 2010). Brain tissue used in these experiments was located in the region between +1.7 to −3.3 mm from bregma.

Whole-cell tissue homogenization

To obtain whole cell extracts, ipsilateral and contralateral brain tissue was homogenized in whole cell lysis buffer containing the following: 50 mM Tris pH 8, 150 mM NaCl, 0.1% SDS, 1% Igepal CA-630, 1 mM PMSF, and a Complete Mini protease inhibitor cocktail (Roche Diagnostics, Indianapolis, IN). Briefly, tissue was disrupted using a handheld electric homogenizer and allowed to incubate on ice for 10 min. Tissue lysates were vortexed and pipetted to break up nuclei. Protein extracts were snap frozen and stored at −80 °C.

Nuclear fractionation

Extraction of nuclear and cytosolic fractions for use in electrophoretic mobility shift assay (EMSA) experiments was performed as previously described (Dignam et al. 1983). Nuclear and cytosolic tissue fractions were snap frozen and stored at −80 °C.

Primary neuronal culture

Primary neurons were isolated and cultured as described previously (Katnik et al. 2006; Davis et al. 2017). Cells were treated with 2 μM cytosine-β-D-arabinofuranoside (Sigma-Aldrich; St. Louis, MO) at 5 days post-isolation to suppress proliferation of glial cells.

Oxygen-glucose deprivation

In vitro ischemia was achieved via oxygen-glucose deprivation (OGD) as previously described (Hall et al. 2009; Rowe et al. 2010; Davis et al. 2017). After 24 h, cells were removed from the chamber and supernatants were collected. Cells were washed twice with PBS and either fixed for 10 min in 4% paraformaldehyde in phosphate buffer or pelleted via centrifugation and snap-frozen prior to storing at −80 °C. Fixed cells were used for immunohistochemical staining and frozen cells were used for RNA extraction.

Lactate dehydrogenase assay

Measurement of lactate dehydrogenase (LDH) in the cellular supernatant was performed as previously described according to the manufacturer's protocol (Davis et al. 2017) using the LDH Cytotoxicity Detection Kit (Takara Biosciences, Madison, WI).

Promoter analysis

Identification of TF binding sites was performed as previously described (Rowe, Leonardo et al. 2010) using Genomatix Software (Munich, Germany). The sequences for the rat

(*Rattus norvegicus*) SOD3 gene was used in the search query and a table was generated for all TF sites. Consensus sites for the TFs in the table were aligned with the rat SOD3 promoter sequence to identify their locations.

siRNA-mediated gene silencing

MZF-1 siRNA was used to suppress its expression in primary cortical neuronal cultures. Neurons were isolated and transfected with MZF-1 siRNA or Control-A siRNA (Santa Cruz Biotechnology, Santa Cruz, CA) using the as previously described (Gärtner et al. 2006; Davis et al. 2017).

Isolation of total RNA

Total RNA was isolated from primary cortical neurons using the Qiagen RNeasy Mini Kit (Valencia, CA) as previously described according to the manufacturer's protocol (Rowe, Leonardo et al. 2010). RNA samples were immediately converted to cDNA or stored at −80 °C.

Real-time PCR

Two-step real-time PCR was performed as previously described to measure in vitro changes in MZF-1 mRNA (Rowe, Leonardo et al. 2010, Davis et al. 2017). Cycle threshold values from the gene of interest and housekeeping gene (18 s rRNA) were used to calculate the relative change in gene expression.

Immunohistochemical analysis

3, 3- diaminobenzidine immunohistochemistry was performed as previously described on fixed primary cultured neurons (Rowe, Leonardo et al. 2010, Davis et al. 2017). Neurons were labeled with rabbit anti-MZF-1 antibodies (1:500; Abcam, San Francisco, CA; RRID:AB_1139620). Biotinylated goat anti-rabbit secondary antibodies (1:300; Vector Laboratories, Burlingame, CA; RRID:AB_2313606) were used for visualization. Coverslips were dried and coverslipped with DPX mounting medium (BDH Laboratories, Poole, England). Images were captured using a Zeiss AxioCam color camera attached to a Zeiss AxioSkop2 microscope (Thornwood, NY) interfaced with ZEN 2 Imaging Software.

Fluorescent immunohistochemistry was performed on brain tissue sections using a previously described protocol (Hall et al. 2009). The following antibodies were used: rabbit anti-MZF-1 (1:500; Abcam, San Francisco, CA;

RRID:AB_1139620), mouse anti-SOD3 4G11G6 (1:250; Novus Biologicals) and mouse anti-neuronal nuclear antigen (NeuN) (1:500; EMD Millipore, Billerica, MA; RRID:AB_2298772) antibodies. AlexaFluor® 488-conjugated goat α-rabbit AlexaFluor® 594-conjugated goat anti-rabbit antibodies (1:250; Life Technologies, Carlsbad, CA; RRID:AB_2576217;) were used for visualizing antigens. Tissue sections were dried and coverslipped with DPX mounting medium. Images were captured using a C2+ Confocal Microscope System (Nikon Instruments Inc., Melville, NY) interfaced with NIS-Elements C software.

Western blot analysis

Western blotting was used for semi-quantitative measurement of protein expression using a previously described procedure (Davis et al. 2017). Samples from ipsilateral brain tissue were run on 10% SDS-PAGE gels. Contralateral tissue served as an internal negative control for the ischemic injury. Membranes were probed with rabbit anti-MZF-1 antibodies (1:250; Abcam; RRID:AB_1139620). Membranes were incubated in IRDye 800CW goat anti-rabbit antibodies (1:20,000; Li-Cor; RRID:AB_2651127) for detection of protein bands. Membranes were visualized using the Odyssey CLx Imaging System (Li-Cor). Membranes were reprobed with mouse anti-β-actin (1:5000; Novus Biologicals; RRID:AB_1216153) and IRDye 680RD goat anti-mouse antibodies (1:20,000; Li-Cor; RRID:AB_10956588).

Electrophoretic mobility shift assay

Electrophoretic mobility shift assays (EMSAs) were performed using Odyssey IRDye® 680RD-labeled consensus oligonucleotides (Integrated DNA Technologies, Coralville, IA) and identical unlabeled nucleotides were obtained from Affymetrix (Santa Clara, CA). The following consensus sequence was for and MZF-1: 5′ AGTGGGGAAGTGGG GAAGTGGGGA 3'

EMSAs were performed as described in the protocol described in the Supplementary Methods online (Li-Cor, Lincoln, NE). Contralateral tissue was included alongside ipsilateral tissue to serve as an internal negative control for the ischemic injury.

To confirm the specificity of the interaction between the labeled oligonucleotides and their respective TFs, unlabeled oligonucleotides were added in excess to the binding reaction prior to adding the labeled

Table 1 Location and sequences of all MZF-1 binding sites in the rat *SOD3* gene promoter

Start position	End position	Strand (±)	Sequence
13	23	+	aaGGGGaacta
46	56	+	gtGGGGacaat
73	83	+	ggGGGGaaagg
368	378	+	ggGGGGaggag

oligonucleotides. To further confirm the specificity of binding, antibodies complementary to MZF-1 (RRID:AB_1139620) were added to the binding reaction in order to either induce a supershift or disrupt the binding reaction between the TF and the labeled oligonucleotides.
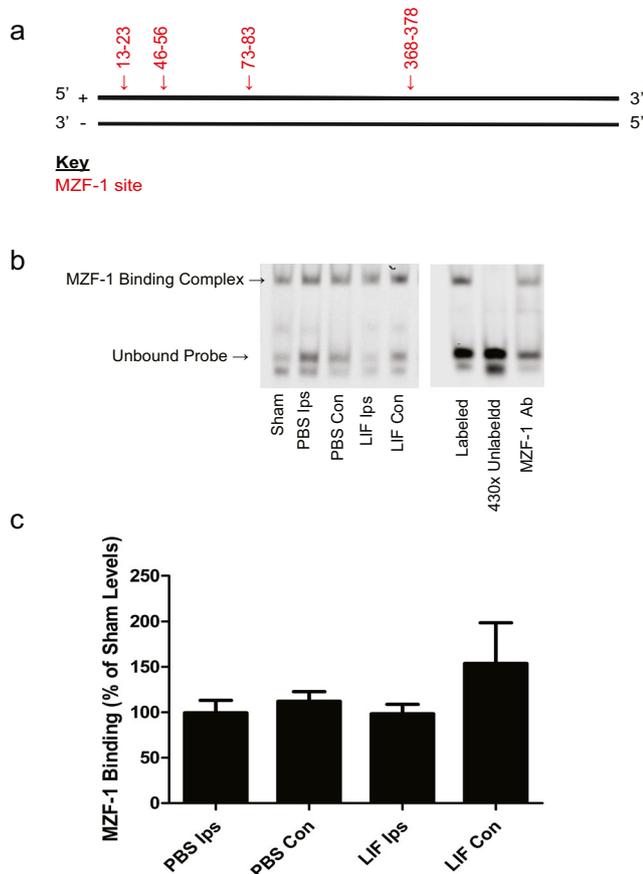

Fig. 1 MZF-1 is Transcriptionally Active in Brain Tissue. **a** Locations of MZF-1 binding sites identified by Genomatix in the rat *SOD3* promoter. **b** Supershift assays confirmed the specificity of MZF-1 binding. **c** Probe/ Protein complexes were quantified by measuring the optical densities corresponding bands. $n = 4$ samples per group. Ips; ipsilateral, Contra; contralateral
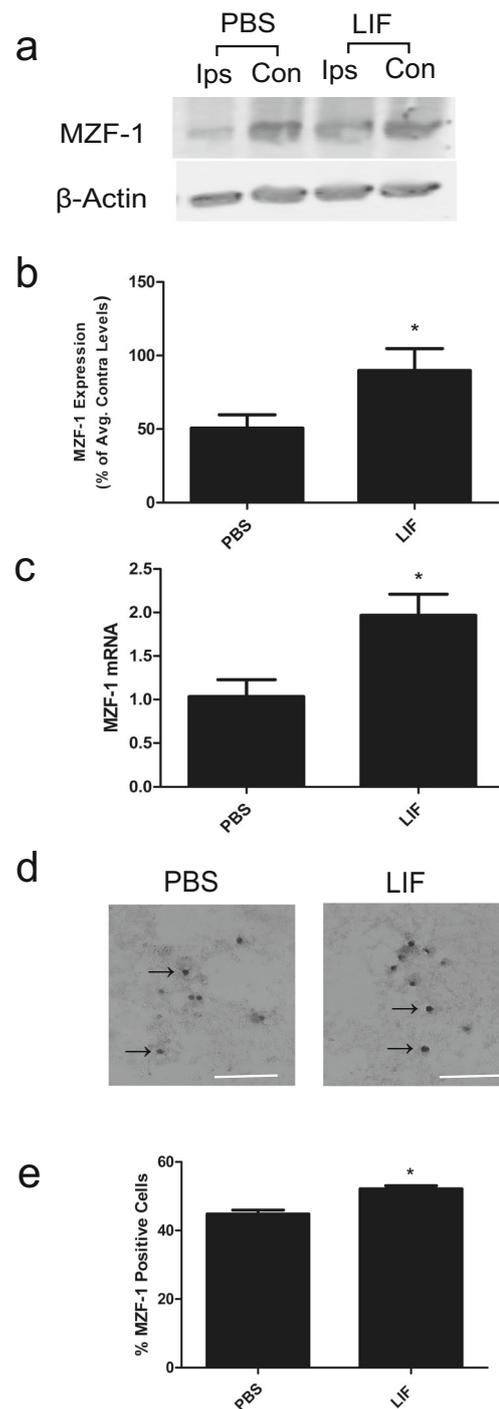
Fig. 2 LIF Treatment Increases MZF-1 Expression in vivo and in vitro. **a–b** Normalized MZF-1 protein levels were significantly increased in the ipsilateral brain tissue of LIF-treated rats compared to those of PBS-treated rats (*$p < 0.05$). $n \geq 5$ samples per group. **c** Cultured treated with 200 ng/ml LIF prior to OGD showed significantly higher levels of MZF-1 mRNA compared to PBS-treated neurons. $n = 3$ wells per group ($p = 0.05$; **d–e**). MZF-1 immunoreactivity was significantly increased after LIF treatment in cultured neurons compared to PBS-treated cells (*$p < 0.05$). $n = 5$ wells per group

Fig. 3 MZF-1 Accumulates in Nuclei of Cortical Neurons after MCAO and LIF Treatment. Tissue sections were labeled with MZF-1 (red) and neuronal nuclear antigen (NeuN; green) antibodies to visualize localization of MZF-1 in neuronal nuclei. Arrows identify representative cells. Scale bars = 50 μm
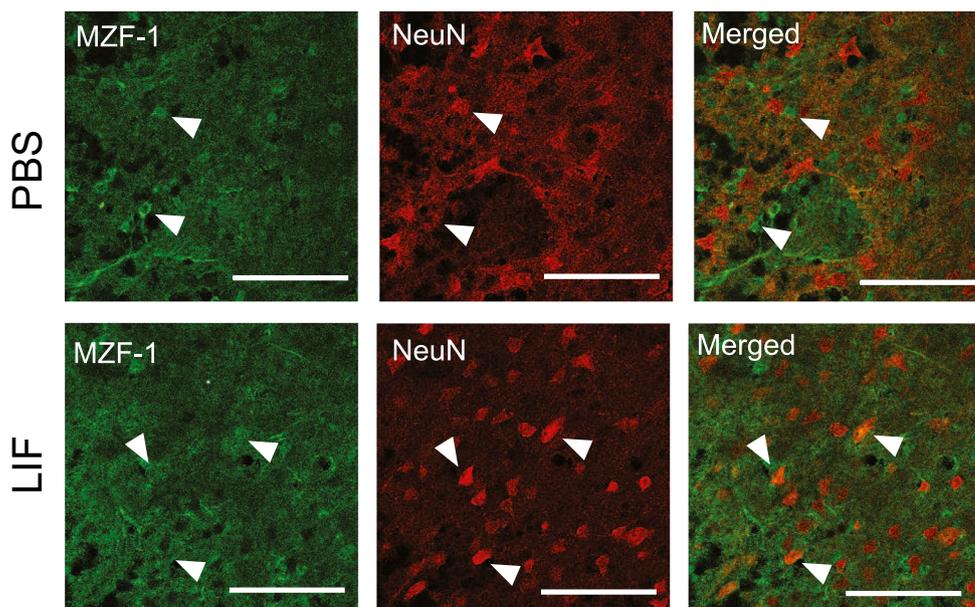
Data analysis

Data values are expressed as the mean ± the standard error of the mean. Images were minimally processed in a uniform manner across treatment groups and were analyzed using ImageJ software (NIH, Bethesda, MD). Statistical analysis for experiments containing two groups was performed using a Mann-Whitney U test and a Kruskal-Wallis test was used for those containing three or more groups. To detect outliers, the interquartile method was used as previously described (Rousseeuw and Hubert 2011). Detected outliers based on this criterion were removed for analysis of Fig. 3e to prevent significant effects from being masked by skewed data. A p value

≤0.050 was considered significant. All p values reported are one-tailed.

Results

MZF-1 is transcriptionally active in the ischemic brain

Within the rat *SOD3* promoter, four MZF-1 sites were identified. The locations of these binding sites are found in Table 1. A visual diagram showing the locations of these sites is found in Fig. 1a. Supershift assays performed using antibodies against MZF-1 disrupted formation of the MZF-1/probe

Fig. 4 SOD3 co-localizes with MZF-1 after LIF treatment. Tissue sections were labeled with antibodies against MZF-1 (red) and SOD3 (green) to show co-localization in brain tissue. Arrows identify representative cells. Scale bars = 50 μm
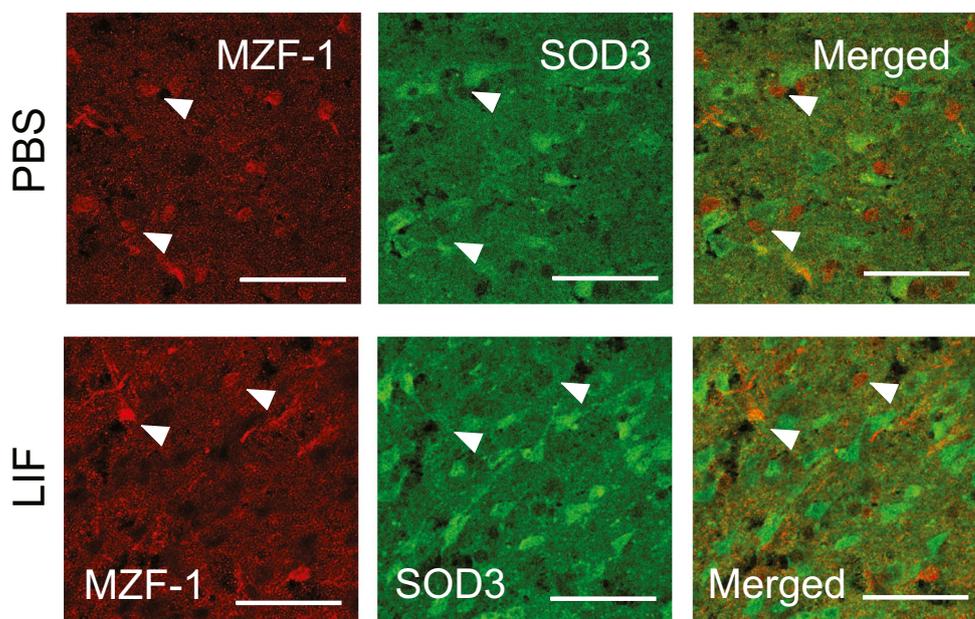
complex (Fig. 1b). The results of the EMSA showed no significant difference in MZF-1 binding activity between PBS- and LIF-treated ipsilateral and contralateral tissue ($p = 0.5378$; H = 2.338; Fig. 1c).

LIF Promotes Upregulation of MZF-1 in vivo and in vitro

MZF-1 protein expression in the ipsilateral tissue were normalized to the average MZF-1 expression in the contralateral tissue of each treatment group. The normalized MZF-1 levels were significantly increased after LIF treatment compared to rats that were treated with PBS after MCAO ($p = 0.0411$; U = 5.000; Fig. 2a and b).

Real-time PCR analysis was used to measure the change in MZF-1 mRNA levels in neurons that were treated with LIF prior to 24 h of OGD. The PCR results confirmed a significant upregulation of MZF-1 mRNA after LIF treatment compared to PBS-treated neurons ($p = 0.0500$; U = 0.000; Fig. 2c).

The percentage of cultured neurons that stained positive for MZF-1 was calculated by dividing by the total number of cells imaged. Neurons that were treated with LIF prior to OGD showed a significant increase in the percentage of MZF-1-positive cells compared to the cells that were treated with PBS ($p = 0.0143$; U = 0.0000; Fig. 2d and e).

MZF-1 co-localizes with neuronal nuclei and SOD3 in vivo

Sections from rats euthanized at 72 h post-MCAO were double-labeled with antibodies against MZF-1 (red), and NeuN (green). MZF-1 immunoreactivity was also observed in the nuclear and cytosolic regions of cortical cells in animals from both treatment groups (Fig. 3).

Tissue sections from PBS and LIF-treated rats were also stained with SOD3 and MZF-1 antibodies. Co-localization of SOD3 (green) with MZF-1 (red) was observed after PBS and LIF treatment (Fig. 4).

## MZF-1 siRNA counteracts in vitro neuroprotection by LIF

MZF-1 siRNA was used suppress MZF-1 expression immediately following isolation. Transfected neurons were treated with PBS or LIF (200 ng/ml) and subjected to 24 h of OGD.. There was a significant difference in LDH release among neurons transfected with scrambled and MZF-1 siRNA and treated with LIF after 24 h OGD ($p = 0.0273$; H = 7.41). Furthermore, there was a 176% increase in LDH release between neurons transfected with scrambled siRNA and treated with LIF and neurons transfected with MZF-1 siRNA and treated with LIF (Fig. 5).
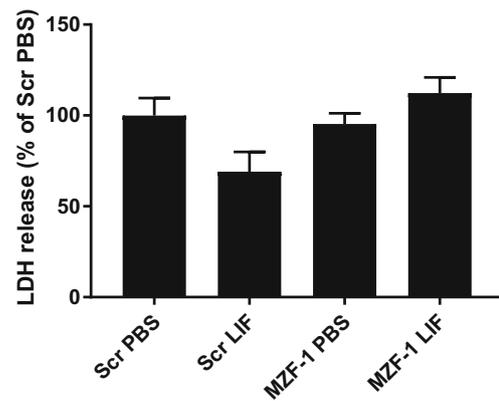
Fig. 5 MZF-1 siRNA counteracts LIF-mediated neuroprotection in vitro. Lactate dehydrogenase (LDH) activity was used to measure cellular death after 24 h OGD. LIF treatment and transfection with MZF-1 siRNA significantly altered LDH release after OGD (*$p < 0.05$). $n = 3$–4 wells per group

Discussion

To our knowledge this is the first report to show that MZF-1 is directly involved with survival signaling in neurons. Previously, MZF-1 has been associated with gene regulation in immune and hematopoietic cells (Hromas et al. 1991); Hromas et al. 1996a, b #5977; Hui, 1995 #5983;
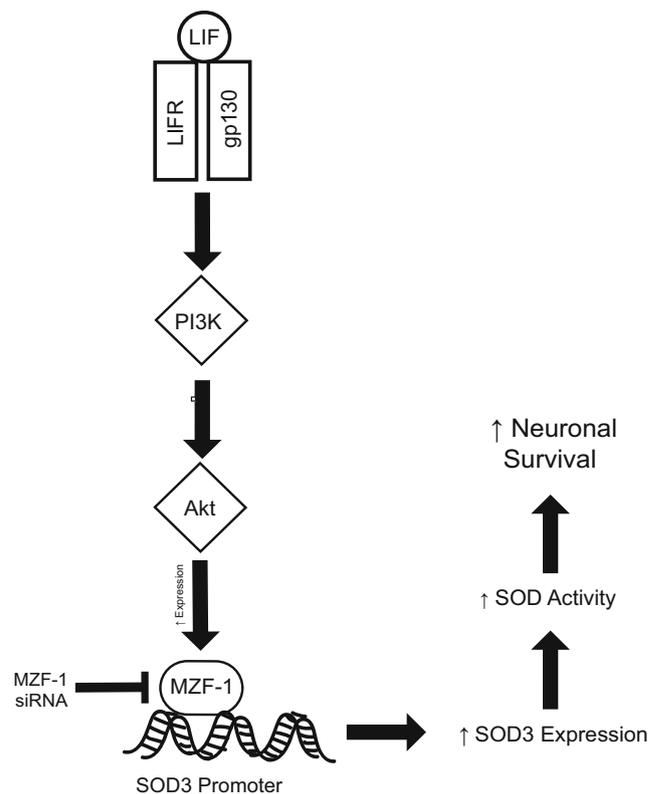
Fig. 6 LIF promotes neural cell survival through MZF-1 transcriptional activity. Upon binding to its receptor, LIF increases Akt signaling, which increases downstream transcriptional activity of TFs, including MZF-1

Robertson, 1998 #4608}. MZF-1, which belongs to the Kruppel family of TFs and is highly expressed by cells of myeloid origin, (Hromas et al. 1991) modulated expression of several genes that play various roles in stroke pathogenesis/recovery (Morris et al. 1995; Hromas et al. 1996b). Apomorphine stimulated upregulation of fibroblast growth factor-2, a neuroprotective factor, in astrocytes through MZF-1 activity (Luo et al. 2009). MZF-1 binding sites were identified in the promoter region for peroxiredoxin I, a member of the peroxiredoxin family that is highly expressed by oligodendrocytes (Mizusawa et al. 2000; Kim et al. 2008). In addition, levels of matrix metalloproteinase 2, a gelatinase released by activated microglia during stroke, was significantly decreased by overexpressing MZF-1 in the SiHa cervical cancer line (Tsai et al. 2012). Other groups showed that increasing PI3K/Akt signaling may increase levels of MZF-1. For instance, calcitriol regulates CD11b and CD14 expression in mononuclear cells by upregulating MZF-1 protein levels in a PI3K-dependent manner (Moeenrezakhanlou et al. 2008). Granulocyte/macrophage colony stimulating factor, a cytokine implicated in leukocyte maturation, increases neuronal survival through PI3K/Akt activation (Takahashi et al. 2006; Schabitz et al. 2007). In addition, Hui et al. demonstrated that granulocyte/macrophage colony-stimulating factor, which signals through Akt, increases levels of MZF-1 (Hui et al. 1995).

Oh et al. reported that LIF binding to its receptor activates the PI3K/Akt pathway (Oh et al. 1998). Furthermore, Akt signaling regulates the activity of TFs such as MZF-1, which regulate the expression of protective genes during stroke (Rowe et al. 2010, 2012). SOD3, which increases total SOD activity and promotes antioxidant protection in the ischemic brain, is a crucial protective gene induced by LIF. Furthermore, Genomatix identified MZF-1 binding sites within the rat *SOD3* gene. This current report establishes MZF-1 as a key regulator of LIF-induced protective signaling during ischemia (Fig. 6).

The identification of a novel transcription factor that plays a role in LIF-mediated neuroprotection allows for the continued evaluation of LIF as a preclinical stroke therapeutic. Knowing the mechanism of cellular protection for LIF in this model provides valuable insight regarding its potential as a treatment for stroke in humans. Further studies warrant the investigation of pharmaceutical agents that increase the activity of MZF-1 after stroke, as well as the identification of new protective genes under the transcriptional control of MZF-1. Although the mechanisms underlying the regulation of these transcription factors during LIF treatment are not entirely understood, these data provide information on a new neuroprotective pathway as and a target for stroke treatments.

Compliance with ethical standards

Conflict of interest None

Publisher's Note Springer Nature remains neutral with regard to jurisdictional claims in published maps and institutional affiliations.

References

Ajmo CT Jr, Vernon DO, Collier L, Pennypacker KR, Cuevas J (2006) Sigma receptor activation reduces infarct size at 24 hours after permanent middle cerebral artery occlusion in rats. Curr Neurovasc Res 3(2):89–98

Azari MF, Galle A, Lopes EC, Kurek J, Cheema SS (2001) Leukemia inhibitory factor by systemic administration rescues spinal motor neurons in the SOD1 G93A murine model of familial amyotrophic lateral sclerosis. Brain Res 922(1):144–147

Barber PA, Demchuk AM, Zhang J, Buchan AM, A. S. Group (2000) Validity and reliability of a quantitative computed tomography score in predicting outcome of hyperacute stroke before thrombolytic therapy. Lancet 355(9216):1670–1674

Butzkueven H, Zhang JG, Soilu-Hanninen M, Hochrein H, Chionh F, Shipham KA, Emery B, Turnley AM, Petratos S, Ernst M, Bartlett PF, Kilpatrick TJ (2002) LIF receptor signaling limits immune-mediated demyelination by enhancing oligodendrocyte survival. Nat Med 8(6):613–619

Davis SM, Collier LA, Leonardo CC, Seifert HA, Ajmo CT, Pennypacker KR (2017) Leukemia inhibitory factor protects neurons from ischemic damage via upregulation of superoxide dismutase 3. Mol Neurobiol 54(1):608–622

Dignam JD, Lebovitz RM, Roeder RG (1983) Accurate transcription initiation by RNA polymerase II in a soluble extract from isolated mammalian nuclei. Nucleic Acids Res 11(5):1475–1489

Dirnagl U, Iadecola C, Moskowitz MA (1999) Pathobiology of ischaemic stroke: an integrated view. Trends Neurosci 22(9):391–397

Fukui S, Ookawara T, Nawashiro H, Suzuki K, Shima K (2002) Post-ischemic transcriptional and translational responses of EC-SOD in mouse brain and serum. Free Radic Biol Med 32(3):289–298

Gärtner A, Collin L, Lalli G (2006) Nucleofection of primary neurons. Methods Enzymol 406:374–388

Goyal M, Menon BK, van Zwam WH, Dippel DWJ, Mitchell PJ, Demchuk AM, Dávalos A, Majoie CBLM, van der Lugt A, de Miquel MA, Donnan GA, Roos YBWEM, Bonafe A, Jahan R, Diener H-C, van den Berg LA, Levy EI, Berkhemer OA, Pereira VM, Rempel J, Millán M, Davis SM, Roy D, Thornton J, Román LS, Ribó M, Beumer D, Stouch B, Brown S, Campbell BCV, van Oostenbrugge RJ, Saver JL, Hill MD, Jovin TG (2016) Endovascular thrombectomy after large-vessel ischaemic stroke: a meta-analysis of individual patient data from five randomised trials. Lancet 387(10029):1723–1731

Hacke W, Kaste M, Bluhmki E, Brozman M, Dávalos A, Guidetti D, Larrue V, Lees KR, Medeghri Z, Machnig T (2008) Thrombolysis

with alteplase 3 to 4.5 hours after acute ischemic stroke. N Engl J Med 359(13):1317–1329

Hall AA, Guyer AG, Leonardo CC, Ajmo CT Jr, Collier LA, Willing AE, Pennypacker KR (2009) Human umbilical cord blood cells directly suppress ischemic oligodendrocyte cell death. J Neurosci Res 87(2): 333–341

Hastrup S, Damgaard D, Johnsen SP, Andersen G (2016) Prehospital acute stroke severity scale to predict large artery occlusion: design and comparison with other scales. Stroke 47(7):1772–1776

Hendriks JJ, Slaets H, Carmans S, de Vries HE, Dijkstra CD, Stinissen P, Hellings N (2008) Leukemia inhibitory factor modulates production of inflammatory mediators and myelin phagocytosis by macrophages. J Neuroimmunol 204(1–2):52–57

Hromas R, Collins SJ, Hickstein D, Raskind W, Deaven LL, O'Hara P, Hagen FS, Kaushansky K (1991) A retinoic acid-responsive human zinc finger gene, MZF-1, preferentially expressed in myeloid cells. J Biol Chem 266(22):14183–14187

Hromas R, Boswell S, Shen RN, Burgess G, Davidson A, Cornetta K, Sutton J, Robertson K (1996a) Forced over-expression of the myeloid zinc finger gene MZF-1 inhibits apoptosis and promotes oncogenesis in interleukin-3-dependent FDCP.1 cells. Leukemia 10(6): 1049–1050

Hromas R, Davis B, Rauscher F III, Klemsz M, Tenen D, Hoffman S, Xu D, Morris J (1996b) Hematopoietic transcriptional regulation by the myeloid zinc finger gene, MZF-1. Molecular Aspects of Myeloid Stem Cell Development. Springer, New York, pp 159–164

Hui P, Guo X, Bradford PG (1995) Isolation and functional characterization of the human gene encoding the myeloid zinc finger protein MZF-1. Biochem 34(50):16493–16502

Ip NY, Nye SH, Boulton TG, Davis SM, Taga T, Li Y, Birren SJ, Yasukawa K, Kishimoto T, Anderson DJ, Stahl N, Yancopoulos GD (1992) CNTF and LIF act on neuronal cells via shared signaling pathways that involve the IL-6 signal transducing receptor component gp130. Cell 69(7):1121–1132

Katnik C, Guerrero WR, Pennypacker KR, Herrera Y, Cuevas J (2006) Sigma-1 receptor activation prevents intracellular calcium dysregulation in cortical neurons during in vitro ischemia. J Pharmacol Exp Ther 319(3):1355–1365

Kim JH, Bogner PN, Baek SH, Ramnath N, Liang P, Kim HR, Andrews C, Park YM (2008) Up-regulation of peroxiredoxin 1 in lung cancer and its implication as a prognostic and therapeutic target. Clin Cancer Res 14(8):2326–2333

Leonardo CC, Pennypacker KR (2011) The splenic response to ischemic stroke: what have we learned from rodent models? Transl Stroke Res 2:328–338

Leonardo CC, Hall AA, Collier LA, Ajmo CTJ, Willing AE, Pennypacker KR (2010) Human umbilical cord blood cell therapy blocks the morphological change and recruitment of CD-11b-expressing isolectin-binding proinflammatory cells after middle cerebral artery occlusion. J Neurosci Res 88(6):1213–1222

Luo X, Zhang X, Shao W, Yin Y, Zhou J (2009) Crucial roles of MZF-1 in the transcriptional regulation of apomorphine-induced modulation of FGF-2 expression in astrocytic cultures. J Neurochem 108(4): 952–961

Madsen TE, Melluzzo S, Wira CR, Magdon-Ismail Z, Day D, Gropen T, Investigators NCC (2017) Minorities, women, and stroke belters left behind in t-PA use despite quality improvement efforts. Stroke 48(suppl_1):A116–A116

Marriott MP, Emery B, Cate HS, Binder MD, Kemper D, Wu Q, Kolbe S, Gordon IR, Wang H, Egan G, Murray S, Butzkueven H, Kilpatrick TJ (2008) Leukemia inhibitory factor signaling modulates both central nervous system demyelination and myelin repair. Glia 56(6): 686–698

McMeekin P, White P, James MA, Price CI, Flynn D, Ford GA (2017) Estimating the number of UK stroke patients eligible for endovascular thrombectomy. Eur Stroke J 2(4):319–326

Mizusawa H, Ishii T, Bannai S (2000) Peroxiredoxin I (macrophage 23 kDa stress protein) is highly and widely expressed in the rat nervous system. Neurosci Lett 283(1):57–60

Moenrezakhanlou A, Shephard L, Lam L, Reiner NE (2008) Myeloid cell differentiation in response to calcitriol for expression CD11b and CD14 is regulated by myeloid zinc finger-1 protein downstream of phosphatidylinositol 3-kinase. J Leukoc Biol 84(2):519–528

Morris J, Davis B, Klemsz M, Xu D, Tenen D, Hromas R (1995) The myeloid zinc finger gene, MZF-1, regulates the CD34 promoter in vitro. Blood 86(10):3640–3647

Oh H, Fujio Y, Kunisada K, Hirota H, Matsui H, Kishimoto T, Yamauchi-Takihara K (1998) Activation of phosphatidylinositol 3-kinase through glycoprotein 130 induces protein kinase B and p70 S6 kinase phosphorylation in cardiac myocytes. J Biol Chem 273(16): 9703–9710

Powers WJ, Rabinstein AA, Ackerson T, Adeoye OM, Bambakidis NC, Becker K, Biller J, Brown M, Demaerschalk BM, Hoh B (2018) 2018 guidelines for the early management of patients with acute ischemic stroke: a guideline for healthcare professionals from the American Heart Association/American Stroke Association. Stroke 49(3):e46–e99

Rousseeuw PJ, Hubert M (2011) Robust statistics for outlier detection. Wiley Interdiscip Rev Data Min Knowl Discov 1(1):73–79

Rowe DD, Leonardo CC, Hall AA, Shahaduzzaman MD, Collier LA, Willing AE, Pennypacker KR (2010) Cord blood administration induces oligodendrocyte survival through alterations in gene expression. Brain Res 1366:172–188

Rowe DD, Leonardo CC, Recio JA, Collier LA, Willing AE, Pennypacker KR (2012) Human umbilical cord blood cells protect oligodendrocytes from brain ischemia through Akt signal transduction. J Biol Chem 287(6):4177–4187

Rowe DR, Collier LA, Seifert HA, Chapman CB, Leonardo CC, Willing AE, Pennypacker KR (2014) Leukemia inhibitory factor promotes functional recovery and oligodendrocyte survival in rat models of focal ischemia. Eur J Neurosci 40:3111–3119

Schabitz WR, Kruger C, Pitzer C, Weber D, Laage R, Gassler N, Aronowski J, Mier W, Kirsch F, Dittgen T, Bach A, Sommer C, Schneider A (2007) A neuroprotective function for the hematopoietic protein granulocyte-macrophage colony stimulating factor (GM-CSF). J Cereb Blood Flow Metab 28(1):29–43

Seifert HA, Leonardo CC, Hall AA, Rowe DD, Collier LA, Benkovic SA, Willing AE, Pennypacker KR (2012) The spleen contributes to stroke induced neurodegeneration through interferon gamma signaling. Metab Brain Dis 27(2):131–141

Smith WS, Sung G, Saver J, Budzik R, Duckwiler G, Liebeskind DS, Lutsep HL, Rymer MM, Higashida RT, Starkman S (2008) Mechanical thrombectomy for acute ischemic stroke: final results of the multi MERCI trial. Stroke 39(4):1205–1212

Strålin P, Karlsson K, Johansson BO, Marklund SL (1995) The interstitium of the human arterial wall contains very large amounts of extracellular superoxide dismutase. Arterioscler Thromb Vasc Biol 15(11):2032–2036

Suzuki S, Yamashita T, Tanaka K, Hattori H, Sawamoto K, Okano H, Suzuki N (2005) Activation of cytokine signaling through leukemia inhibitory factor receptor (LIFR)/gp130 attenuates ischemic brain injury in rats. J Cereb Blood Flow Metab 25(6):685–693

Takahashi K, Hayashi N, Kaminogawa S, Ra C (2006) Molecular mechanisms for transcriptional regulation of human high-affinity IgE receptor beta-chain gene induced by GM-CSF. J Immunol 177(7): 4605–4611

Talwalkar A, Uddin, S, N. C. f. H. Statistics (2015) Trends in Emergency Department Visits for Ischemic Stroke and Transient Ischemic Attack: United States, 201–2011, US Department of Health and Human Services, Centers for Disease Control and Prevention, National Center for Health Statistics

Tsai SJ, Hwang JM, Hsieh SC, Ying TH, Hsieh YH (2012) Overexpression of myeloid zinc finger 1 suppresses matrix metalloproteinase-2 expression and reduces invasiveness of SiHa human cervical cancer cells. Biochem Biophys Res Commun 425(2):462–467

Zelko I, Folz R (2003) Myeloid zinc finger (MZF)-like, Kruppel-like and Ets families of transcription factors determine the cell-specific expression of mouse extracellular superoxide dismutase. Biochem J 369:375–386

Zelko IN, Folz RJ (2004) Sp1 and Sp3 transcription factors mediate trichostatin A-induced and basal expression of extracellular superoxide dismutase. Free Radic Biol Med 37(8):1256–1271

Zelko IN, Mariani TJ, Folz RJ (2002) Superoxide dismutase multigene family: a comparison of the CuZn-SOD (SOD1), Mn-SOD (SOD2), and EC-SOD (SOD3) gene structures, evolution, and expression. Free Radic Biol Med 33(3):337–349